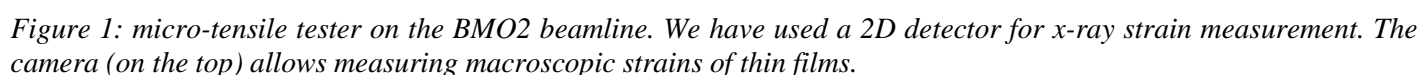


**Date of report:**  
25/08/2009

Received at ESRF:

LMP Phymat, Université Poitiers, Bâtiment SP2MI, Boulevard Marie et Pierre Curie, 86  
962 Futuroscope Chasseneuil Cedex



The substrates used to deposit the gold films were 127.5 mm thick Kapton dog-bone substrates; the in-plane sample dimensions were 14×6 mm. The substrate was cleaned with ethanol before deposition. Metallic films were deposited by physical vapor deposition, i.e. continuous ion beam sputtering. The total thickness of the films was between 20 and 800 nm.

Diffractive methods allows a selective assessment of crystalline phases and crystallographic planes of materials. Thus, this technique is very powerful to study elastic anisotropy effects in polycrystalline materials (selective study of different diffracting planes). The uniaxial tensile device is a Deben tensile tester equipped with a load cell enabling the force measurement with a precision of 0.1 N. Moreover, it is very light (about 500 g) and not cumbersome (90×60×30 mm). During continuous loading, diffraction response has been recorded to determine the elastic strains in thin films.

X-ray experiments combining both reflection and transmission modes were carried out, as described in [2]. This mode is called reflection–transmission mode, as one part of the signal is also studied in transmission thanks to the X-ray transparency of the substrate. In this geometry, strain information is obtained for a given set of direction, i.e. a given set of  $(\Phi, \Psi)$  positions, where  $\Phi$  and  $\Psi$  are the so-called diffraction angle. With a single exposure, this acquisition strategy suffices to perform strain measurements in the three-dimensional space.

The samples were mounted with an angle  $\omega$  (angle between the sample surface and the incident beam direction) of 14° or 18° (dependent of studied films) (Figure 2) with an energy of 20 keV. No absorption correction has been added as we are measuring the relative shift of the Bragg peaks via the shift of the center of the fitted function. The distance between the sample and the detector was set to 123 mm, which corresponds to the minimum distance available in the presence of the beam stop. Moreover, Si powder was placed on the backside of the sample, close to the measuring point, in order to correct for the sample drift during loading. We used Si powder because it offers a sufficient number of diffraction rings at angles covering the whole detector surface. Diffraction patterns on the Si powder were taken at each load step.

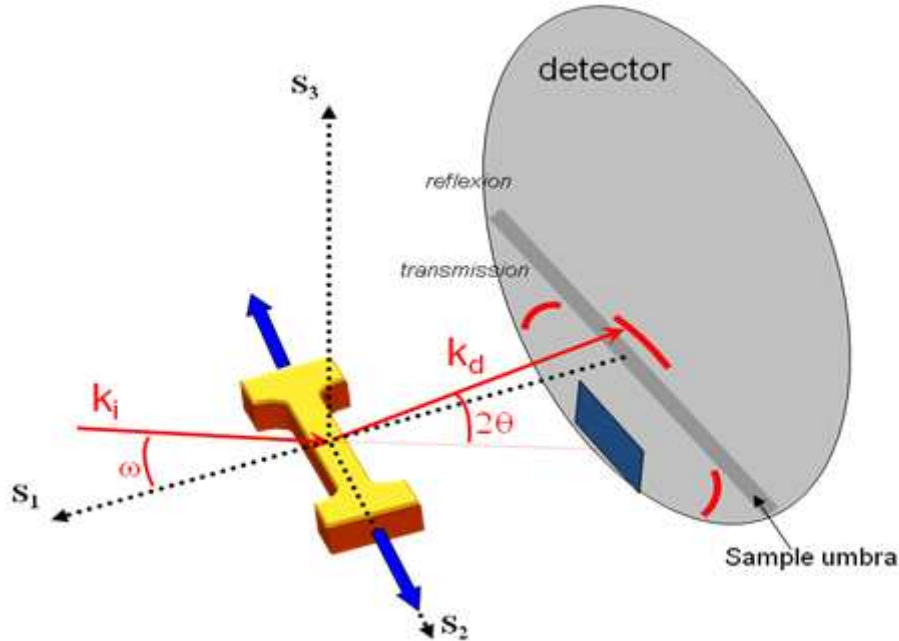


Figure 2: Setup used to record the diffractogram patterns during the in situ tensile tests for the reflexion-transmission mode on the BM02 beamline at ESRF.

Because of the geometry of the experiment and the transparency of the substrate to X-rays, we catch two types of signals on the CCD images. The diffraction patterns (Figure 3) show partial Debye rings, which are continuous for the Si powder and with intensity variations for the Ni thin film (because of the fiber texture). The right part of the image shows the reflected signal from the sample, while the left part shows the transmitted signal. As the silicon powder signal and metallic films signal are recorded at the same time, Si powder rings were used to calibrate the geometrical parameters of the experiment, assuming that the wavelength of the X-ray beam remains stable. Using fit2d (ESRF program) on silicon rings, the sample-to-detector distance as well as the image center and the detector nonorthogonality were calibrated. We have

already noted that the distance may change for the first load steps. When the applied force reaches a few Newtons, the distance remains stable until the end of the experiment. Using the calibrated geometry parameters (center, distance and tilt angle) the data were distributed into  $1^\circ \delta\Psi$  bins and integrated azimuthally in a process referred to as ‘caking’ in the fit2d lexicon. Figure 4 shows an image at this step of the procedure. The reduced data were saved to obtain, for each load step, the classical  $2\theta$ –intensity diagram for each bin, which contains 166 diagrams per load step.

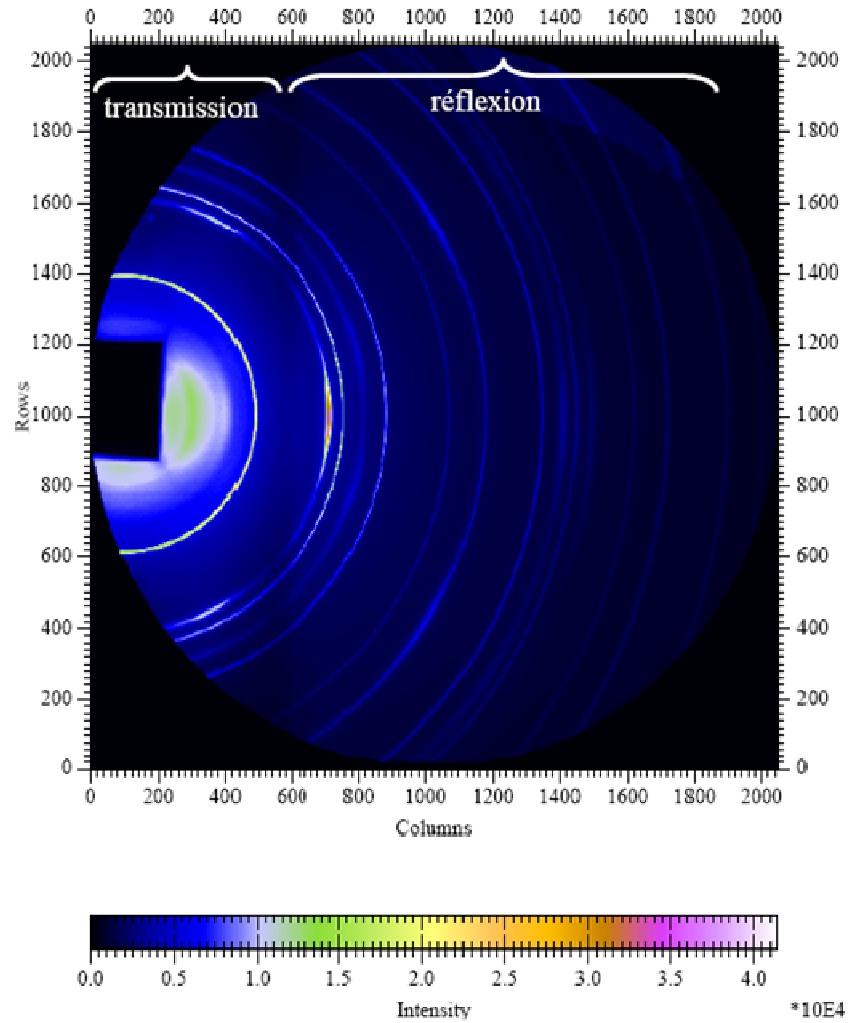


Figure 3: Whole diffraction pattern in the reflection–transmission geometry. The figure shows Ni peak details in the reflection and transmission parts of the image. The sample umbra allows the distinction between the two parts.

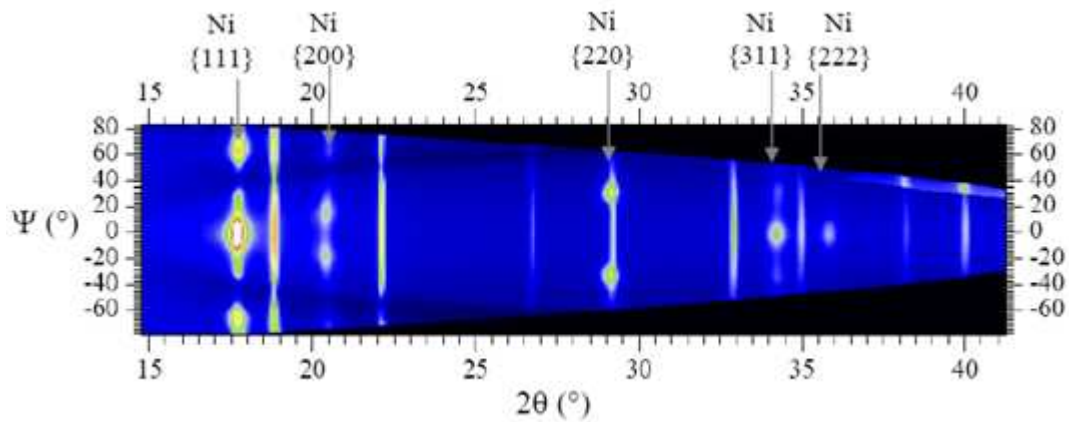


Figure 4: Image of the data reduced by fit2d ( $2\theta$ ,  $\Psi$ , intensity) in the transmission geometry for a 200 nm thick Ni films. It is clear here that intensity varies with  $\Psi$  because of  $\{111\}$  fiber texture of Nickel films

Another in-house program was used to generate inputs for gnuplot in order to fit the Si peaks that are complete over the ring and  $\{111\}$  Au peaks. The code allows us to localize the peak and to extract its

parameters, so that the adjustment procedure in gnuplot using a Pearson VII function starts with parameters close to the final solution. Keeping  $\Psi$  constant, parameters from a previous adjustment are passed to the next load step in the gnuplot script. The parameters extracted from each peak adjustment are the position, intensity, FWHM, shape factor and background polynomial forms (which can be of degrees 0–6). At the end of this procedure, all the parameters for the metallic films and Si peaks are collected for each load step and for each  $\Psi$  position (166 in total).

An example (200 nm thick Nickel film) of results is given in Figure 5. The elastic deformation for the {111} reflexion is plotted as a function applied load, for 5 different  $\Psi$  positions. The response is linear, as expected for linear elasticity, and depends on  $\Psi$  positions. Since the elastic fields are complexes, deformation can be positive or negative, depending on the measurement direction. The positions  $\Psi=0^\circ$  and  $\Psi=44^\circ$  correspond respectively to the strongest and the weakest nickel peak intensity for the {111} reflexion. This is the reason why the dispersion for  $\Psi=44^\circ$  is relatively high as compared to other positions. The whole experimental results will be compared to micro-mechanical models as in references [3]. Moreover, we have planned to study evolution of magnetic properties of Ni films during tensile tests, by using Brillouin Light Scattering (BLS) combined *in situ* with the micro-tensile tester, and thus to compare BLS results with the diffraction ones to extract some magneto-elastic coefficients (a PhD work will start in january 2010). To conclude, performing a complete *in situ* mechanical property analysis of polycrystalline thin films using X-ray diffraction is time consuming with most standard diffraction beamlines at synchrotron facilities and not realistic with laboratory diffractometers. Two-dimensional detection is shown to enable relatively fast and reliable X-ray strain measurements during *in situ* tensile testing of gold films deposited on polyimide substrates.

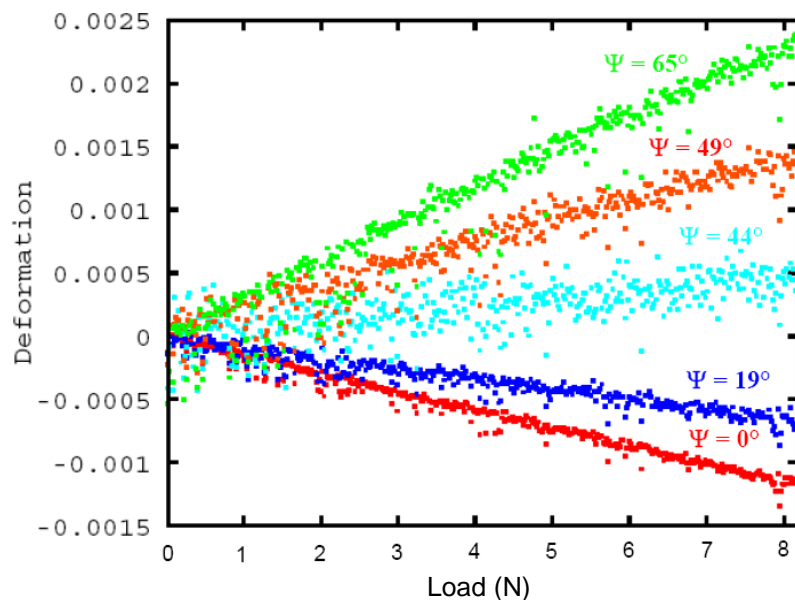


Figure 5: Deformation measured by x-ray diffraction as a function of applied load, for different  $\Psi$  positions.

- [1] D. FAURIE, P. -O. RENAULT, E. LE BOURHIS, P. GOUDEAU  
“Study of texture effect on elastic properties of Au thin films by x-ray diffraction and *in-situ* tensile testing”,  
*Acta Materialia* 54, 4503 (2006)
- [2] G. GEANDIER, P. -O. RENAULT, SIMON TEAT, E. LE BOURHIS, B.LAMONGIE, P. GOUDEAU  
“Benefits of two-dimensional detectors for synchrotron X-ray diffraction studies of thin film mechanical behavior”, *J. Appl. Cryst.* 41, 1076-1088 (2008)
- [3] D. FAURIE, O. CASTELNAU, P. -O. RENAULT, R. BRENNER, E. LE BOURHIS, P. GOUDEAU, G. PATRIARCHE  
“Elastic behavior of polycrystalline thin films inferred from *in-situ* micromechanical testing and modelling”,  
*Appl. Phys. Letters* 89, 061911 (2006)